

# Emergence, Exploration and Learning of Embodied Behavior\*

Yasuo Kuniyoshi, Shinsuke Suzuki and Kyosuke Shiozumi  
Laboratory for Intelligent Systems and Informatics,  
Department of Mechano-Informatics,  
School of Information Science and Technology,  
The University of Tokyo  
Tokyo, Japan  
Email: kuniyosh@isi.imi.i.u-tokyo.ac.jp

September 14, 2005

## Abstract

A novel model for dynamic emergence and adaptation of embodied behavior is proposed. A musculo-skeletal system is controlled by a number of chaotic elements, each of which driving a muscle based on local sensory feedback. Thus, the chaotic elements interact with each other through the physical body and the environment. This overall structure is modelled as a *coupled chaotic system*, which has been known in the complex systems science for its capability of creating and moving among extremely rich variety of ordered patterns. In our model, body-environment interaction dynamics, or *embodiment*, serves as the chaos coupling field, which is non-linear and time-varying. Theoretically very little is known about such cases, but since the coupling field directly reflects the current body-environment dynamics, we believe that the emergent ordered patterns correspond to useful motor coordination patterns which immediately get reorganized in response to dynamically changing environmental situation. We implemented the above model and carried out a series of experiments using a dynamics simulator. The results confirmed the above conjecture. In a “muscle-joint” model and a “multi-legged insect” model, the systems autonomously explored and found meaningful motor behaviors within a few seconds. And when the environmental condition changes they immediately created novel motor patterns which comply with the new situation. Unlike existing learning methods, our model does not require long training period or well-designed reward function. The emergence and adaptation takes place immediately, and yet effective in the current embodied situation. Furthermore, we present a methodology to introduce “goal-directedness” to the system without destroying its emergent property.

---

\*Due to page limitations, this version of the paper presents only partial results (learning part is omitted). A revised and enhanced version will be submitted for final publication.

# 1 Introduction

Real world is full of unexpected contingencies and opportunities. Even at the level of physical motion such as legged locomotion, it is very hard to design appropriate controllers for all possible terrain conditions under uncertain perturbations or even partial mechanical defects. Traditional model-based approach and trajectory planning with feedback control has a strong limitation in this aspect.

Alternatively, adaptive methodologies such as reinforcement learning and genetic algorithm has been actively investigated and successfully applied to real robots. However, they require vast number of trials before converging onto appropriate behaviors or control laws. And once the bodily or environmental condition changes, they need thousands of trials again to adapt to it. Moreover, these methodologies require careful design of evaluation functions which is not always straightforward unless the characteristics of the body and the environment is well understood.

In this paper, we propose a novel model of *immediate* behavior adaptation in response to unpredicted dynamic changes in bodily and environmental situation. If a behavior is generated by some fixed control or by searching to optimize some fixed evaluation function, the above goal is hard to achieve. Rather than control or optimization, we should exploit emergence of consistent motoric patterns from embodied interaction dynamics.

Importance of emergent behavior from embodied interactions has been established [3]. It has been shown that an important effect of embodiment is imposing consistent structures in sensory-motor patterns. However, methodologies for capturing such patterns relied on hebbian neural learning or evolutionary methodologies, requiring a large number of trials.

In the context of dynamic motion control, exploitation of the inherent task dynamics has been successfully applied to juggling [5] and other periodical tasks. When an adaptive neural system is coupled with such natural dynamics, even a complicated body exhibits very robust and flexible behavior as a result of mutual entrainment. One such example is neural oscillator based biped walking [8]. However, in all the successful examples so far, the system stays within a single limit cycle dynamics. Its robustness is limited to attractor dynamics and has no capability of switching to different consistent dynamics.

We propose a novel model in which a distributed set of chaotic elements are coupled with the multi-element musculo-skeletal system. Consistent motor behavior patterns emerge from embodied interactions. The same principle gives rise to immediate adaptation capability with switching to different/novel motion patterns. It requires no training or evaluation function. The system autonomously explores, discovers, and adopts possible motion patterns.

In the following sections, we first present our model of behavior emergence. There we describe the underlying theory called *coupled chaotic system* and show how it can be adopted for a model of embodied behavior emergence. The coupled chaotic system has been known in the complex systems science for its capability of creating and moving among extremely rich variety of ordered patterns.

Our model of behavior emergence is quite simple. However, its behavior is extremely complex. Even theoretically, a behavior of coupled chaotic systems with time-varying non-linear coupling is very poorly understood. Moreover, there has been no attempt so far to exploit this phenomena for robotic behavior generation. Therefore, our emphasis in this paper is to investigate the following points through a series of experiments.

1. How to design the connection between the body and the chaotic elements?
2. How does the system behave in case the structure of body dynamics changes?
3. How does the system behave in case the structure of environment changes?
4. How can we impose “goal-directedness” onto the behavior while maintaining the emergent property?

We present a series of experiments using a dynamics simulator. Concrete interface parameters and systematic investigation of resulting behavior patterns will be given. The results confirmed the above conjecture; In a “muscle-joint” model and a “multi-legged insect” model, the systems autonomously explored and found meaningful motor behaviors within a few seconds. And when the environmental condition changes they immediately created novel motor patterns which comply with the new situation.

Furthermore, we present a methodology to introduce “goal-directedness” to the system without destroying its emergent property.

## 2 A model of emergence from a coupled chaotic system

### 2.1 Coupled chaotic system

Coupled Map Lattice(CML) and Globally Coupled Map(GCM)[2] have been investigated in complex systems science for their rich dynamics properties. They follow (1)-(2). CML is a coupled chaotic system with local interaction (1). GCM is one with global interaction (2).

$$x_{n+1}^i = (1 - \varepsilon) f(x_n^i) + \frac{\varepsilon}{2} \{f(x_n^{i+1}) + f(x_n^{i-1})\} \quad (1)$$

$$x_{n+1}^i = (1 - \varepsilon) f(x_n^i) + \frac{\varepsilon}{N} \sum_{j=1}^N f(x_n^j) \quad (2)$$

Where,  $x_n^i$  denotes the internal state of  $i$ th element at time  $n$ ,  $N$  the total number of elements, and  $\varepsilon$  the connection weight between elements.  $f(x)$  can be any chaos function. In this paper, we adopt a standard *logistic map* represented as the following.

$$f(x) = 1 - ax^2 \quad (3)$$

With no interaction between the elements, all of them behave chaotically.

But with interaction, depending on the parameters  $(a, \varepsilon)$ , variety-rich dynamical structures emerge such as ordered phases (generates clusters in which elements oscillate simultaneously) and partially ordered phases (configuration of clusters changes with times).

This phenomenon is essentially caused by a competition of two tendencies; (1) A tendency to synchronize each other by the effect of the mean-field, and (2) a tendency to take arbitrarily different values due to the nature of chaos dynamics.

## 2.2 Body and environment as an interaction field of chaotic elements

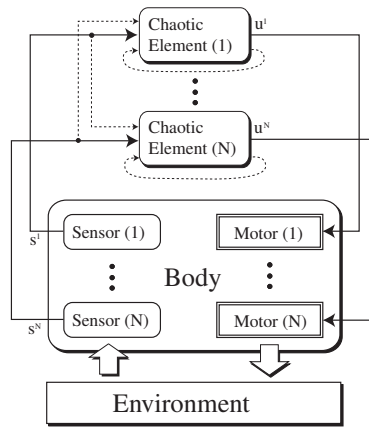


Figure 1: Outline of our model

Figure 1 shows our model of chaos coupling through robotic embodiment.

$N$  chaotic elements are connected with actuators and sensors of the robot body. Each element drives a corresponding actuator based on its current internal state. The effect of  $N$  actuators collectively change the physical state of the body under the constraints and the effects of the environment. In other words, the output of  $N$  chaotic elements are mixed together and transformed by the embodied dynamics. The result is then sensed at each site of the actuator, e.g. in terms of joint angle or muscle length. Each sensor value is then input to the corresponding chaotic element. Then each element updates, by chaotic mapping, its internal state from the new sensor value and the previous internal state.

The important points of our model are as follows :

- There are interactions and mutual entrainments among the dynamics of the chaos system, the body (musculo-skeletal system) and the environment.

- Having a chaotic element connect each sensor and actuator, the whole system is organized as a coupled chaotic system.
- The body and the environment serve as the interaction field for the chaotic elements.

In our model, body-environment interaction dynamics, or *embodiment*, serves as the chaos coupling field, which is non-linear and time-varying. Theoretically very little is known about such cases, but since the coupling field directly reflects the current body-environment dynamics, we believe that the emergent ordered patterns correspond to useful motor coordination patterns which immediately get reorganized in response to dynamically changing environmental situation.

We devised 3 types of formula to update the internal state of an element : (4), (5), and (6). Where,  $u$  denotes the internal state,  $s$  the sensor value, and  $\bar{s}$  the mean of sensor values. The 2nd and the 3rd terms in  $f$  of (4) and (6) are intended to be GCM-like connection and CML-like connection.  $\varepsilon_1, \varepsilon_2$  are the weight of each connection. We used logistic map (3) for  $f(x)$ <sup>1</sup>. Initial condition of  $u$  is a random value within (0, 1).

Table 1 shows the interpretation of each formula <sup>2</sup>.

$$\begin{aligned} \text{Type-A : } u_n^i &= f \left\{ u_{n-1}^i + \varepsilon_1 (\bar{s}_{n-1} - s_{n-1}^i) \right. \\ &\quad \left. + \varepsilon_2 \left( \frac{s_{n-1}^{i+1} + s_{n-1}^{i-1}}{2} - s_{n-1}^i \right) \right\} \end{aligned} \quad (4)$$

$$\text{Type-B : } u_n^i = f(s_n^i) \quad (5)$$

$$\begin{aligned} \text{Type-C : } u_n^i &= f \left\{ s_{n-1}^i + \varepsilon_1 (\bar{s}_{n-1} - s_{n-1}^i) \right. \\ &\quad \left. + \varepsilon_2 \left( \frac{s_{n-1}^{i+1} + s_{n-1}^{i-1}}{2} - s_{n-1}^i \right) \right\} \end{aligned} \quad (6)$$

### 3 Experiments

We use dynamics simulation library ODE[7] to simulate the dynamics of a robot and environment. The time step size of ODE was 0.01 and that of couple chaotic system was  $T_c$ . In implementation,  $u$  and  $s$  in section 2.2 were associated with  $s_{raw}$  and  $m$  ((7), (8), (9), (10)), where  $s_{raw}$  denotes the raw value of a sensor and  $m$  the motor output of an actuator. Note that the gains  $g_u, g_{u_{out}}, g_s, g_{s_{in}}$

---

<sup>1</sup>In implementation, to avoid divergence,  $x$  is constrained as follows :  $if(x > 1) x = 1, if(x < -1) x = -1$

<sup>2</sup>In order to understand the ‘‘adjustment’’ effect, the GCM/CML equations should be transformed by applying  $f$  on both sides and re-arranged to match (4)-(6)

Table 1: Interpretation of the update rules of the coupled chaotic systems

GCM	Each element follows its own pure chaos dynamics with some adjustment to approach the global mean value of all the other pure chaos elements.
CML	Each element follows its own pure chaos dynamics with some adjustment to approach the local mean value of the adjacent pure chaos elements.
Type-A	Each element follows its own pure chaos dynamics with some adjustment to reduce the difference of the corresponding sensor value from the global and the local means of other sensor values.
Type-B	Each element is updated by a chaos map of its sensor value. The sensor value contains the effects of the self and the other elements mixed together through the embodiment. The mixing function does not appear explicitly in the equation. It is a non-linear and time-varying function, reflecting the physical dynamics of the body-environment interaction.
Type-C	In addition to the Type-B, some adjustment is applied in order to reduce the deviation of the corresponding sensor value from the global and the local means of other sensor values.

and the offsets  $o_u, o_{u_{out}}, o_s, o_{s_{in}}$  are independent of the element index  $i$ . They are constant parameters.

$$u_{out} = g_u \cdot u + o_u \quad (7)$$

$$m = g_{u_{out}} \cdot u_{out} + o_{u_{out}} \quad (8)$$

$$s_{in} = g_{s_{in}} \cdot s_{raw} + o_{s_{in}} \quad (9)$$

$$s = g_s \cdot s_{in} + o_s \quad (10)$$

## 3.1 Experiments with a muscle-joint model

### 3.1.1 Configuration

Firstly, we experiment with a muscle-joint model shown in Fig. 2 which consists of two cylindrical rigid bodies and 12 muscle fibers. The base link is fixed to the ground, and the upper link is connected by a ball-joint to the base link. It can be bent in any direction within the limit of 0.5 [rad]. The 12 muscle fibers

are attached between the two links isotropically.

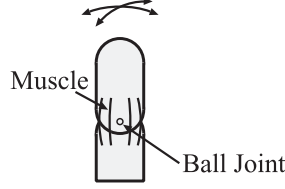


Figure 2: Appearance of the muscle-joint model

Each muscle fiber is modelled with Hill's characteristic equation [4].  $m$  in (8) corresponds to the activation level of a muscle fiber in this model. The sensor value  $s_{raw}$  is provided by either a "length-sensor" measuring the normalized length of the muscle fiber or a "tension sensor"<sup>3</sup> measuring the normalized tension of the muscle fiber. In all experiments,  $(g_{u_{out}}, o_{u_{out}})$  was set to  $(0.5, 0.5)$  respectively. In case of tension sensor,  $(g_{s_{in}}, o_{s_{in}})$  was set to  $(-2.5, 3.0)$ . In case of length sensor,  $(g_{s_{in}}, o_{s_{in}})$  was set to  $(1.0, 0.0)$ .

### 3.1.2 Experiments with/without sensor feedback

Firstly, when there is no sensor feedback (Fig. 3), the motion of the joint was chaotic and no cluster structure was observed.

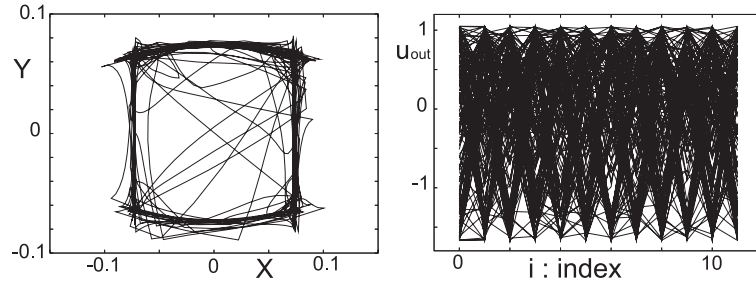


Figure 3: Experiment with no sensor feedback. Trajectory of the center of mass of the upper link projected on  $x - y$  plane (left graph). Cluster plot of the chaotic elements (right). For each element with index  $i$ , its motor output  $u_{out}$  is plotted superposedly for  $n = 10, 11, 12, \dots$ . The points of all the elements are connected with a line for each time step. (Type-A,  $a = 1.6$ ,  $\varepsilon_1 = 0.0$ ,  $\varepsilon_2 = 0.0$ ,  $T_c = 0.21$ ,  $g_u = 1.7$ ,  $g_s = 2.0$ ,  $o_u = -0.65$ ,  $o_s = -1.0$ )

Secondly, in case of an experiment with tension sensor feedback, the motion was chaotic for the initial several steps. But after a time, it changed to the ordered rhythmical motion. Fig. 4 is the graph while the motion was rhythmical. Cluster structure is observed.

<sup>3</sup>In case of tension sensor, before the process of (10),  $s_{in}$  is constrained as follows:  $if(s_{in} > 1) s_{in} = 1$ ,  $if(s_{in} < -1) s_{in} = -1$

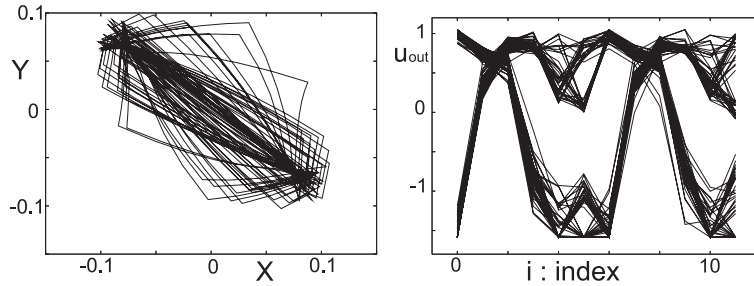


Figure 4: Experiment with feedback of tension sensor (Type-A, tension sensor,  $a = 1.55$ ,  $\varepsilon_1 = 0.3$ ,  $\varepsilon_2 = 0.3$ ,  $T_c = 0.21$ ,  $g_u = 1.7$ ,  $g_s = 2.0$ ,  $o_u = -0.65$ ,  $o_s = -1.0$ )

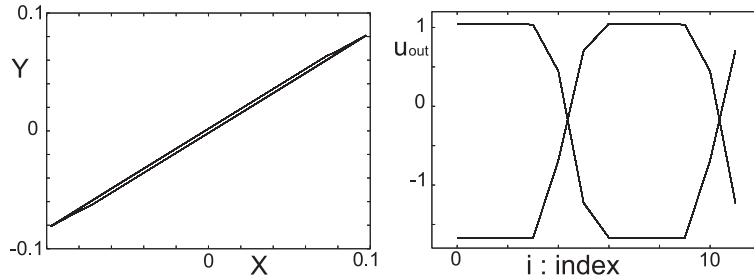


Figure 5: Experiment with feedback of length sensor (Type-B, length sensor,  $a = 1.6$ ,  $T_c = 0.21$ ,  $g_u = 1.7$ ,  $g_s = 1.0$ ,  $o_u = -0.65$ ,  $o_s = 0.0$ )

In case of an experiment with length sensor feedback, the motion was ordered and rhythmical from the beginning (Fig. 5). In the same experiment with a different parameter set, the motion was rhythmical in the beginning, then after a while, the direction of oscillation changed and it began another rhythmical motion (Fig. 6). The change of oscillating direction occurred nonperiodically.

### 3.1.3 Analysis of the system behavior with parameter variations

In order to examine how the system behavior changes with parameter variations, we analyzed the time series of a global variable for various parameter sets. We chose  $(x, y)$ , the coordinates of the center of mass of the top link projected on the base plane, as the global variable representing the behavior characteristic of the entire system. We adopted maximum Lyapunov exponent as the method to analyze the time series<sup>4</sup>.  $(x, y)$  was sampled every time the chaos mapping is applied. Data from 300 steps except for the first 10 steps were used for the analysis. To estimate Lyapunov exponent from time series, we used the nonlinear time series analysis package ‘‘TISEAN’’ [1]. The algorithm to estimate

<sup>4</sup>To put it simply, maximum Lyapunov exponent of chaotic dynamics is positive and that of limit cycle dynamics is zero.



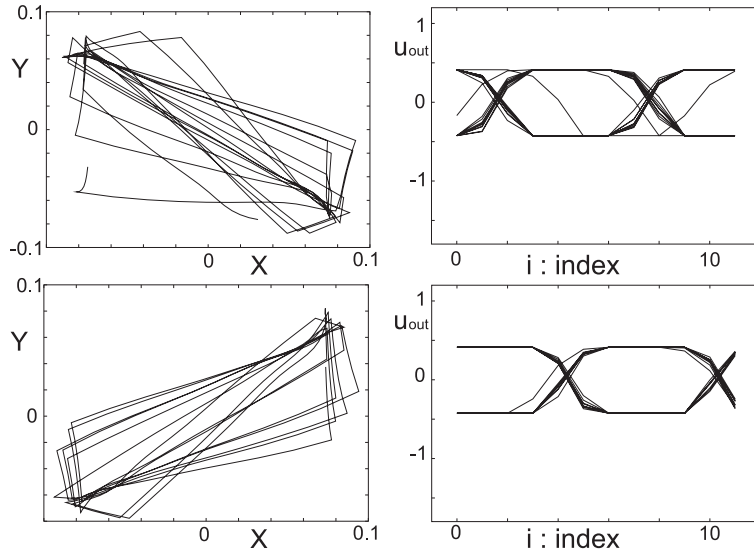


Figure 6: Experiment when dynamic transitions could be seen. The upper graph shows the behavior before transition and the lower one shows that after transition. (Type-A, length sensor,  $a = 1.6$ ,  $T_c = 0.21$ ,  $g_u = 0.52$ ,  $g_s = 1.0$ ,  $o_u = -0.107$ ,  $o_s = 0.0$ )

Lyapunov exponent adopted by this software was the method of Sano-Sawada[6]. We tested 10 different initial conditions for each parameter set and calculated the probability of  $\lambda_{max}$  being zero or negative, where  $\lambda_{max}$  denotes the larger of  $\lambda_x$  and  $\lambda_y$ . Here,  $\lambda_x$  denotes the maximum Lyapunov exponent estimated from the time series of  $x$  and likewise for  $\lambda_y$ .

The upper graph of Fig. 7 shows the probability and the lower one shows orderliness of apparent motion for each parameter set. We tested several patterns of initial condition for each parameter set and categorized the orderliness by qualitative observation as shown in Table 2. The two graphs show a similar structure.

Table 2: Classification based on appearance of motion

A	Stable rhythmic motion appears, and it lasts forever.
B	Rhythmic motion appears, but it sometimes changes into a disorder or transits to another rhythmic pattern.
C	No rhythmic motion appears.

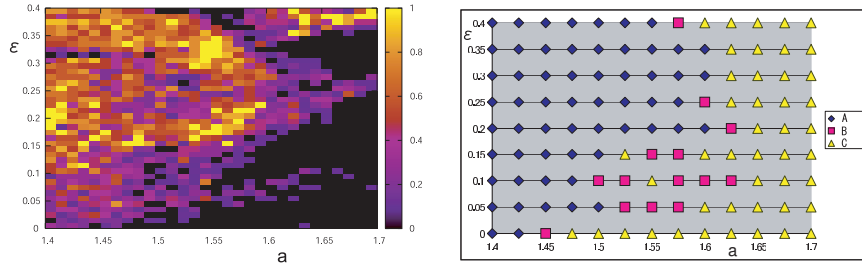


Figure 7: Lyapunov exponent of global variable and orderliness of appearance of motion to “ $a$ ” and “ $\varepsilon$ ”. (Type-A, tension-sensor,  $T_c = 0.21$ ,  $g_u = 1.7$ ,  $g_s = 2.0$ ,  $o_u = -0.65$ ,  $o_s = -1.0$ )

### 3.1.4 Experiments with variations in the body structure

In our model, the body is a interaction field for the chaotic elements. In this experiment, we observed the system’s behavior when the structure of body is changed by adding muscle fibers aligned askew or adding muscle fibers aligned disproportionately (Fig. 8).

In case of an experiment with added muscle fibers aligned askew, depending on the parameter  $a$ , we observed four kinds of motion which could not be seen in case of the original configuration: Around  $a = 1.3$  the joint remained leaning with a small oscillation, around  $a = 1.5$  it alternated the direction of oscillation, around  $a = 1.6$  it made an aperiodic motion, and greater than  $a = 1.7$  it rotated orderly. Fig. 9 shows the result : beginning at the top,  $a = 1.3$ ,  $a = 1.5$ ,  $a = 1.6$ , and  $a = 1.75$ .

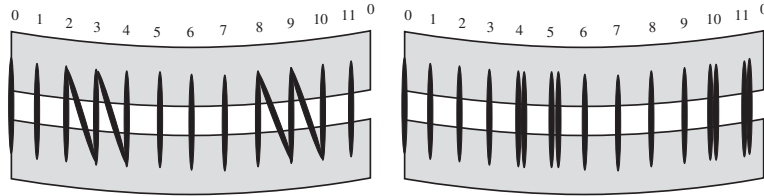


Figure 8: Alignment of muscle fibers (expanded along the circumferential direction)

In case of the experiment with added muscle fibers aligned disproportionately, the direction of oscillation was always from  $(-1, 1)$  to  $(1, -1)$ , while in case of no added muscle fibers the direction varied depending on the initial condition. Fig. 10 shows the result.

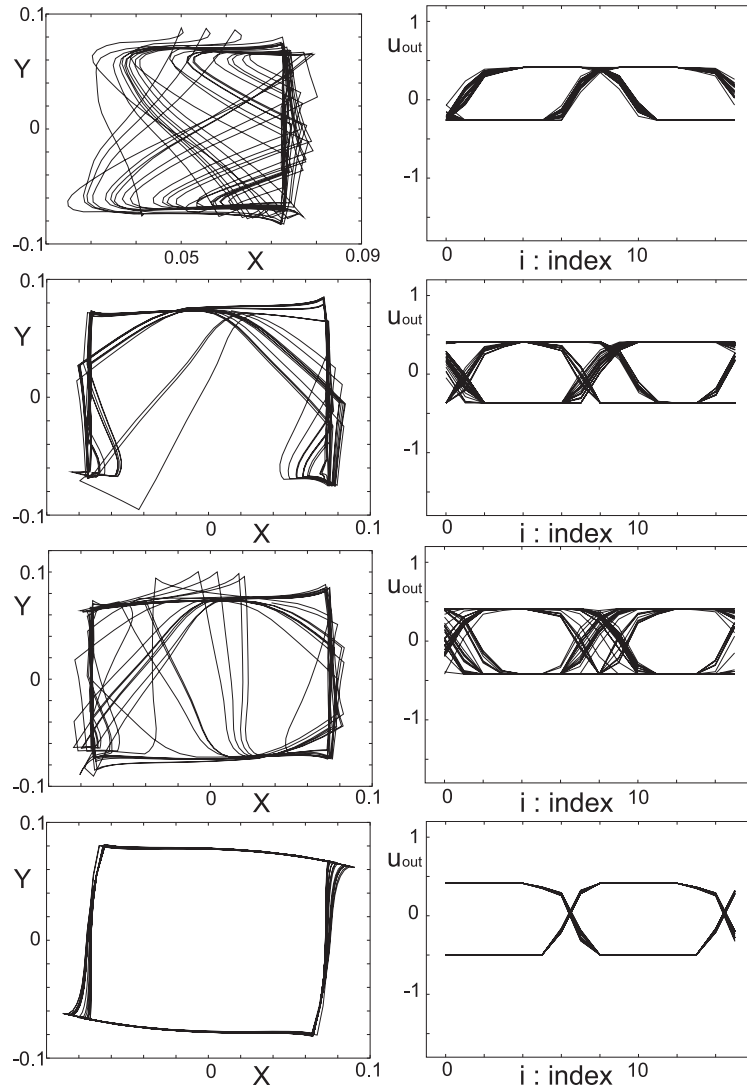


Figure 9: Experiment with added muscle fibers aligned askew (Type-B, length sensor,  $T_c = 0.21$ ,  $g_u = 0.52$ ,  $g_s = 1.0$ ,  $o_u = -0.107$ ,  $o_s = 0.0$ )

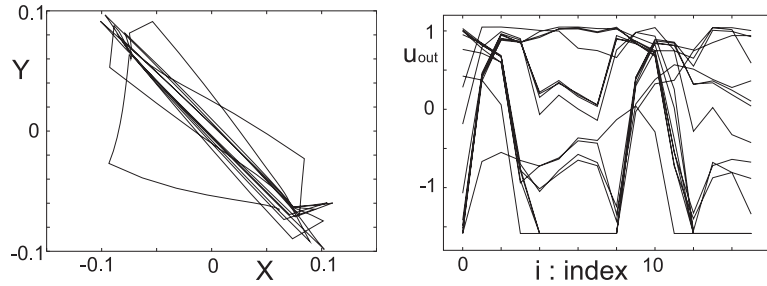


Figure 10: Experiment with added muscle fibers aligned disproportionately (Type-A, tension sensor,  $a = 1.55$ ,  $\varepsilon_1 = 0.3$ ,  $\varepsilon_2 = 0.3$ ,  $T_c = 0.21$ ,  $g_u = 1.7$ ,  $g_s = 2.0$ ,  $o_u = -0.65$ ,  $o_s = -1.0$ )

### 3.1.5 Experiments with a dynamic change of the environmental structure

The environment makes a part of the interaction field for the chaotic elements. In this experiment, we observed the system's behavior when the structure of the environment is dynamically changed by bringing in an obstacle disturbing the oscillation of the muscle-joint system (Fig. 11).

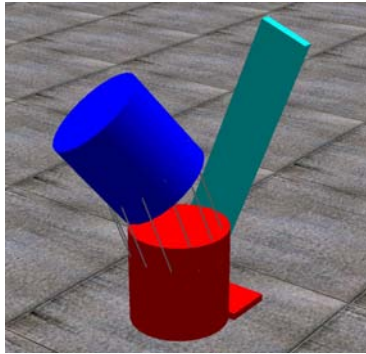


Figure 11: The muscle joint model and obstacle

The obstacle was brought in at  $t = 3$ . Fig. 12 shows the result : beginning at the top, from  $t = 0.42$  to  $t = 3.15$ , from  $t = 3.15$  to  $t = 6.93$ , and from  $t = 6.93$  to  $t = 12.6$ . A little while after colliding against the obstacle, the joint made a complex motion that it repeated colliding in a short period of time and the motor commands were chaotic. But soon after that, within about 3 seconds, it began to oscillate orderly in a new collision-free direction.

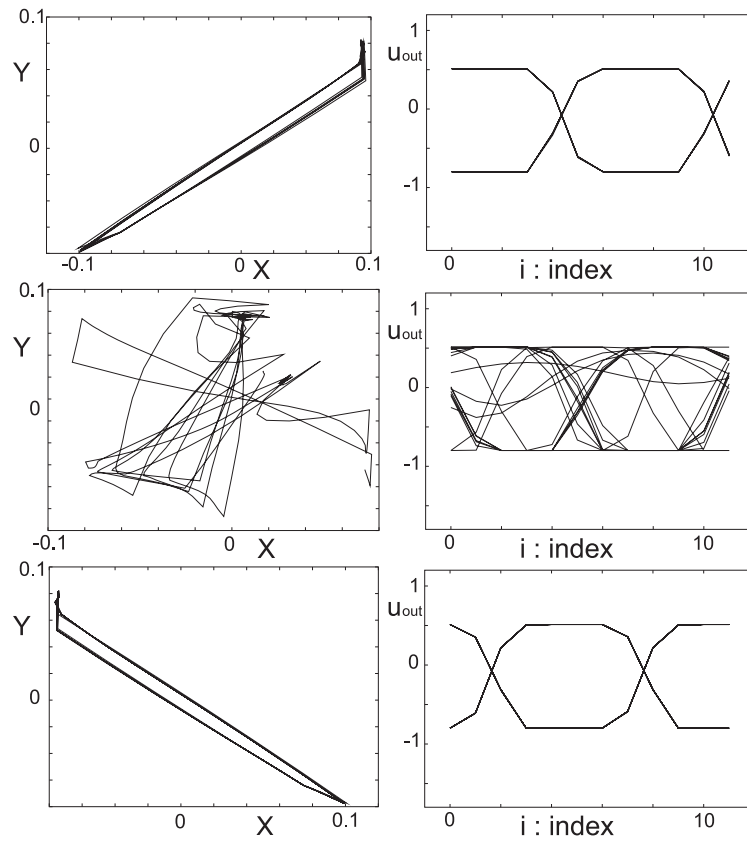


Figure 12: Experiment with obstacle (Type-B, length sensor,  $a = 1.6$ ,  $T_c = 0.21$ ,  $g_u = 0.82$ ,  $g_s = 1.0$ ,  $o_u = -0.3$ ,  $o_s = 0.0$ )

## 3.2 Experiments with an insect-like multi-legged robot

### 3.2.1 Configuration

In order to investigate the effects of our model in a more meaningful behavior with more complex interactions with the environment, we defined an insect-like multi-legged robot. The robot has a disc-shaped body with 12 legs attached on its fringe with regular spacing (Fig. 13). Each leg is connected to the body by a rotational joint and 2 springs whose spring constant is  $K$ . Each leg can swing only in the direction shown in the middle of Fig. 13, and its joint angle is constrained to be less than  $\pm\theta_{lim}$ . The environment has a standard gravity and a constant friction (with the static friction coefficient  $\mu$ ).  $m$  in (8) corresponds to the torque  $\tau$  of each joint.  $s_{raw}$  in (9) corresponds to the angle  $\theta$ . Table 3 shows the parameters common to all the experiments using the above robot model.

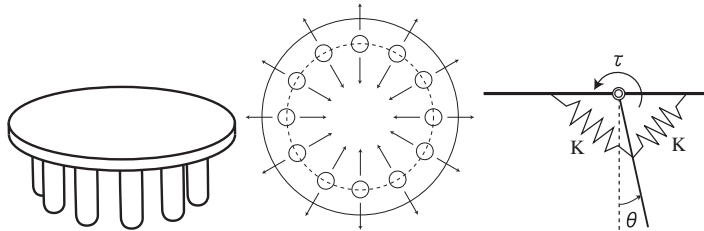


Figure 13: Appearance of the insect-like robot (left), direction of leg motion (middle), and the mechanism of a leg (right).

Table 3: Parameters common to all experiments with the insect-like robot

$T_c$	$K$	$\theta_{lim}$	$g_{uout}$	$g_s$	$g_{sin}$	$o_{uout}$	$o_s$	$o_{sin}$
0.17	1.0	0.8	1.0	0.5	1.25	0.0	0.5	0.0

### 3.2.2 Experiments with sensor feedback

With no sensor feedback, no order was observed in the motion of the robot. It just kept on randomly struggling around the same spot on the ground.

On the other hand, when the sensor feedback is introduced, after the initial chaotic period (a few seconds), the robot started to move in a certain direction, and then finally showed a stable locomotive behavior with a constant speed in a stable direction. The locomotive behavior was realized by synchronizing the 3 or 4 hind legs and kicking the ground with them. Fig. 14 is the graph while the locomotive behavior was observed.

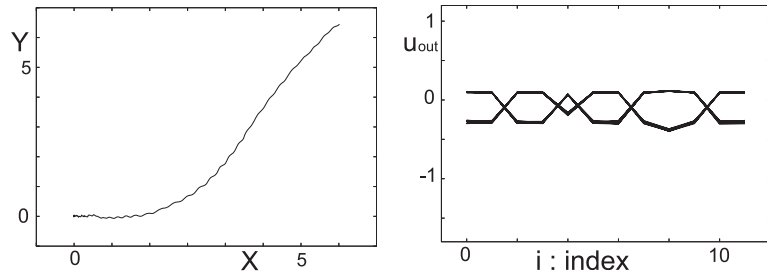


Figure 14: Experiment with sensor feedback (Type-C,  $a = 1.47$ ,  $\varepsilon_1 = 0.1$ ,  $\varepsilon_2 = 0.1$ ,  $g_u = 0.4$ ,  $o_u = -0.28$ ,  $\mu = 0.1$ )

### 3.2.3 Imposing goal-directedness without destructing the emergent property

In this experiment, the configuration was changed as follows.

1. A weight was attached to the body via a hinge joint which was placed above the center of the body and can rotate 360 degrees around the  $z$  axis (Fig. 15).
2. The start position of the robot was  $(0,0)$  on the ground plane, and the goal position was set as  $(-5,-5)$ .
3. The robot is assumed to be able to continuously sense the direction of the goal.
4. The robot drives the hinge joint and moves the weight to the opposite side of the body from the goal (Fig. 15). The robot also freezes the motion of the four legs positioned perpendicular to the orientation of goal.
5. The other legs are actuated in the same way as the previous experiment.

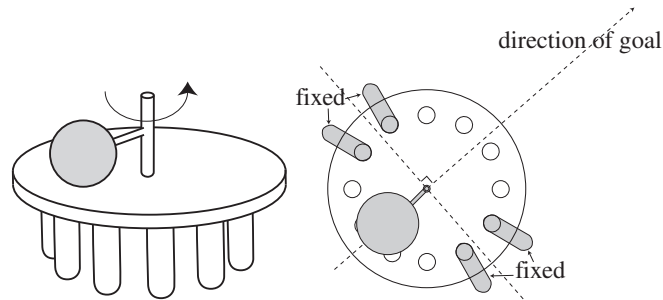


Figure 15: Appearance of the robot and control mechanism to follow objective behavior while maintaining the emergent ability

Fig. 16 shows the result. The robot approached the goal with a gallop-like locomotion. On its way toward the goal the robot sometimes appeared to have

lost the direction temporarily, but then it immediately made some motion in effect of adjusting the direction of movement toward the goal.

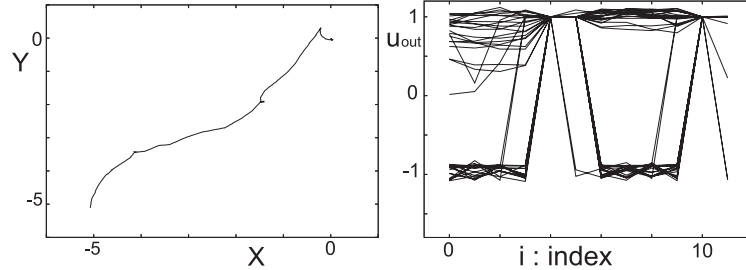


Figure 16: Experiment with the control mechanism designed for the behavior of the whole system to follow the objective behavior (Type-C,  $a = 1.6$ ,  $\varepsilon_1 = 0.3$ ,  $\varepsilon_2 = 0.3$ ,  $g_u = 0.4$ ,  $o_u = -0.28$ ,  $\mu = 0.1$ )

## 4 Summary and Discussions

### 4.1 About the results

**Experiment using a muscle joint model** No ordered motion could be seen in case of no sensor feedback. But ordered rhythmic motion emerged in case of Type-A with tension sensors and in case of Type-B with length sensors.

What happened should be that ordered global patterns emerged from the chaotic elements due to the structural synchronization effect by the interaction field of body and environment. The result appeared as rhythmic motions with compressed degrees-of-freedom. In other words, this took the form of coordinated motion of the multi-degree-of-freedom body.

In comparison with the pure mathematical model of [2], our model is like GCM in that the global variable, i.e. the movement of the upper link, is affected by a collective contribution from all the chaos elements, which is fed back to each element. And it is also like CML in that the fed back value depends on the position of each element in the body. Dynamic transition like Fig. 6 may be related to the characteristic phenomena of coupled chaotic system called “chaotic itinerancy”, discovered by Tsuda et al.

**Analysis of the system behavior parameter variations** Each behavior pattern of the system was persistent over a certain range of area in the parameter space. Fig. 7 also supports in terms of Lyapunov exponent the above observation that the sensitivity of behavior to the parameter sets is low. Here, the maximum Lyapunov exponent indicates the presence of orderliness of motion.

**Experiments with variations in the body structure** In case of the experiment with added muscle fibers aligned askew, various new motion patterns



exploiting the added mode were observed.

In case of the experiment with added muscle fibers aligned disproportionately, the direction in which oscillation emerged was the only direction in which the muscle fibers were added, and the trajectory of the link was more straight than that with no added fibers.

Our interpretation is that the motion emerged from the interaction of chaotic elements reflects the dynamics of the body. In other words, the system automatically generated a new motion adapted to the new body.

### **Experiments with a dynamic change of the environmental structure**

When an obstacle is suddenly introduced against the established motion pattern of the muscle-joint model, a few seconds of struggling followed by a transition to a new collision-free motion pattern was observed. Our interpretation is that the change of the environment destroyed the established motion pattern which allowed other modes of oscillation to dominate. In other words, the system exploited its redundant degrees of freedom which have been suppressed but continuously active in order to instantaneously cope with the new situation. Interestingly, chaotic motion appeared during the transition phase.

The above result provides an example of a very quick adaptation to a change of environment. And it was realized by a simple mechanism of interacting nonlinear dynamics, without any explicit programming of obstacle avoidance.

**Experiments with an insect-like multi-legged robot** The phenomenon that the robot continued moving to a certain direction in spite of its symmetric body structure can be regarded as an emergence of an ordered pattern.

It is also interesting to note that despite of the perfectly symmetric configuration of the body, the individual roles of the legs emerged and differentiated, such as the three or four hind-legs kicking the ground in a coordinated manner.

**Imposing goal-directedness without destructing the emergent property** Generally speaking, “emergence” and “control” have conflicting characteristics. In order to make the robot to move in a particular direction, one might specify a particular trajectory for each leg, making sure that it precisely traces the trajectory. Such a method completely destroys the interaction among the chaotic elements together with the emergence property.

In our experiment, goal-directedness was imposed via a physical process in terms of dynamically changing constraints, e.g. by constraining the motion of some legs and by changing the weight balance of the body. As a result, the entire system exhibited an objective behavior. What happened is that the change of the global parameter and the constraint invoked the immediate adaptation confirmed in the previous experiments, resulting in a meaningful adjustment of the motion pattern via the embodied feedback to each element.

Despite of the imposed constraints, the system still maintains its emergent capability because a majority of the legs stay unconstrained. Hence, emergence and control coexists in this example.

## 4.2 Conclusions

We have presented a novel model of dynamic behavior emergence and adaptation, in which multiple chaos elements are bidirectionally coupled with the multiple degrees of freedom bodies. This model is inspired by pure mathematical models called GCM and CML which are capable of autonomously creating and switching among a rich variety of dynamic patterns.

The original mathematical model assumed a simple averaging of multiple chaos elements in order to make them interact with each other and to dynamically form coherent patterns. In our model, the averaging is replaced by the body-environment interaction dynamics, which is nonlinear and time-varying. Here, the robot body is driven by the collective contribution from the multiple chaos elements under the constraints from the environmental structure, and the resulting body motion is sensed at each degree of freedom, feeding back to each corresponding chaos element. Thus the body-environment dynamics, or *embodiment*, acts as the interaction field for the chaos elements. It maintains the essential effect of mixing and creating a common mode from multiple chaotic signals as the original averaging, but has an additional effect of reflecting the dynamic state of the physical body on the feedback signals which are differentiated depending on each corresponding physical part of the body.

Although rigorous theoretical analysis of the effect of our model is still an open issue, we showed some of its power in several simulation experiments. The simulated robots exhibited the following capabilities:

- Capability of creating and switching coherent motions which appear as appropriate and meaningful for given bodily and environmental structures.
- Capability to immediately adapt to changes in bodily structures and to dynamic changes in the environmental constraints. Unlike other adaptation methods based on learning or evolutionary computation, our system required only a few seconds of struggling before creating a new motion pattern.
- Capability of goal-directed and yet emergent behaviors. This was achieved by carefully imposing a goal-directed effect on the chaos coupling field, or the global dynamics, i.e. the physics of the body.

The above work suggests many important open issues for future research, including applicability to more general body structures, integrating more variety of sensors, pursuing more complicated and meaningful behaviors, integration with learning mechanisms for fixating and combining the acquired motion patterns, and using the proposed model to understand the effect of embodiment more deeply.

## Acknowledgement

This work was supported by Grant-in-Aid for Scientific Research from JSPS, Japan. The authors would like to express their thanks to Prof. Ichiro Tsuda, Prof. Rolf Pfeifer, Prof. Kazuyuki Aihara and many other researchers for the valuable discussions.

## References

- [1] Rainer Hegger, Holger Kantz, and Thomas Schreiber. TISEAN, Nonlinear Time Series Analysis. <http://www.mpipks-dresden.mpg.de/~tisean/>.
- [2] K. Kaneko and I. Tsuda. *Complex Systems: Chaos and Beyond*. Springer, 2001.
- [3] Rolf Pfeifer and Christian Scheier. *Understanding Intelligence*. MIT Press, 1999.
- [4] Nakamura R. and Saito H. *Kisoundougaku*. Ishiyakushuppan, 4 edition, 1992.
- [5] A. A. Rizzi and D. E. Koditschek. Further progress in robot juggling: The spatial two-juggle. In *Proc. IEEE Int. Conf. Robotics and Automation*, pages 919–924, 1993.
- [6] M. Sano and Y. Sawada. Measurement of the lyapunov spectrum from a chaotic time series. *Phys. Rev. Lett.*, 55:1082, 1985.
- [7] Russell Smith. Open dynamics engine(ode). <http://opende.sourceforge.net/ode.html>.
- [8] G. Taga, Y. Yamaguchi, and H. Shimizu. Self-organized control of bipedal locomotion by neural oscillators in unpredictable environment. *Biological Cybernetics*, 65:147–159, 1991.